CORA Cork Open Research Archive
Cartlann Taighde Oscailte Chorcaí

Title	Effects of commercial no-clean flux on reliability of fine pitch flip-chip package with solder bumps and copper pillars
Authors	Wakeel, Saif;Haseeb, A. S. M. A.;Hoon, Khoo Ly;Amalina, M. A.
Publication date	2022-07-15
Original Citation	Wakeel, S., Haseeb, A. S. M. A., Hoon, K. L. and Amalina, M. A. (2022) 'Effects of commercial no-clean flux on reliability of fine pitch flip-chip package with solder bumps and copper pillars', IEEE Transactions on Components Packaging and Manufacturing Technology, 12(8), pp. 1386-1394. doi: 10.1109/TCPMT.2022.3191604
Type of publication	Article (peer-reviewed)
Link to publisher's version	10.1109/TCPMT.2022.3191604
Rights	© 2022, IEEE. Personal use of this material is permitted. Permission from IEEE must be obtained for all other uses, in any current or future media, including reprinting/republishing this material for advertising or promotional purposes, creating new collective works, for resale or redistribution to servers or lists, or reuse of any copyrighted component of this work in other works.
Download date	2026-10-30 07:35:48
Item downloaded from	https://hdl.handle.net/10468/13581

UCC
University College Cork, Ireland
Coláiste na hOllscoile Corcaigh

This article has been accepted for publication in IEEE Transactions on Components, Packaging and Manufacturing Technology. This is the author's version which has not been fully edited content may change prior to final publication. Citation information: DOI 10.1109/TCPMT.2022.3191604

Effects of commercial no-clean flux on reliability of fine pitch flip-chip package with solder bumps and copper pillars

Saif Wakeel, A.S.M.A. Haseeb, *Member, IEEE*, Khoo Ly Hoon, M.A. Amalina

***Abstract*— In this work, two commercial no clean fluxes, namely, extremely low residue no-clean flux (NC-1) and ordinary no-clean flux (NC-2), were used for the preparation of a fine pitch flip-chip package with a 7.6x7.6 mm^2 Si die on a 17x17 mm^2 organic substrate. One water-soluble flux (WS) was also used for comparison. Moisture sensitivity of the package was evaluated using JESD22-A113D (30 ºC/60% relative humidity (RH), 192 hours, 3x reflow at 260 ºC). Thermal cycling tests were performed following JESD22-A104D (-65 ºC to 150 ºC). The high-temperature storage life (HTSL) of the packages was investigated using JESD22-A103C (175 ºC). Underfill delamination or voids in the package were investigated by confocal scanning acoustic microscopy (C-SAM). Failure characteristics of the packages were also studied using scanning electronic microscopy (SEM). After moisture sensitivity level test (MSL) test, vehicles prepared by NC-1 and NC-2 showed failure. SEM images revealed severe delamination between underfill and solder mask in the presence of amine/amide and carboxylic acid based no-clean flux (NCF) residue. Solder bump crack were found at <500 cycles for samples prepared with NC-1 which contains tertiary amine and long carbon chain (C8:C10:C12) carboxylic acid-based. However, failure occurred at <1500 cycles for NC-2 containing secondary amide and shorter carbon chain length (C3) carboxylic acid. Samples prepared using WS did not show any failure for up to 2000 cycles. Thus, NCF treated assemblies performed poorly in moisture sensitivity and temperature cycling tests.**

***Index Terms*— No-clean flux; thermal cycling; moisture sensitivity; high temperature storage life; reliability analysis; underfill delamination.**

I. Introduction

IN recent years, few studies have been performed on the moisture sensitivity level (MSL) of the flip-chip package using no-clean flux (NCF). This test was done under different levels of temperature and humidity as per JESD22-A113D [1]-[5]. Results of these studies showed that underfill epoxy absorbed moisture under humidity conditions. Also, in presence of hygroscopic and non-dissolvable residue, moisture was absorbed by residue in certain locations. This hindered the adhesion of underfill to those locations then after 3 times reflow in MSL, the moisture expanded (popcorning) and became voids thereby, leading to package failure. Thermal cycling tests have been done for flip-chip package employing NCF by following JESD22-A104D [6]-[13]. It has been found that solder bump deformed at the opposite side of underfill dispense due to non-dissolvable residue of NCF which hindered the adhesion of underfill around solder bump. This increased the thermal stress transfer to solder bump which finally ended with deformation under temperature cycling conditions [7]. Also, flux residue that was dissolvable in underfill reduced the glass transition temperature which may soften the underfill during thermal cycling thus, leading to solder bump failure [7]. Limited studies have been conducted on thermal storage reliability of flip-chip package in presence of NCF residue as per JESD22-A103C [10], [13]. Results of these studies revealed that no solder bump crack and resistance failure occurred after 1500 hours, and IMC thickness was thicker than time zero.

Previous studies reported on the failure of NCF treated flip-chip packages in moisture sensitivity, thermal cycling, and high-temperature storage tests [1]-[13]. However, no attention has so far been paid as to how the constituents of NCF and their characteristics affect the reliability. Such characteristics include hygroscopicity, carbonyl functional group and carbon chain length of weak organic acid (WOA) activators, and reactivity of adhesion promoter amines. In recent years, in addition to conventional NCF, some companies started developing extremely low residue NCF. But no work has reported the effects of extremely low residue NCF on the reliability of fine pitch flip-chip package. Also, most of the published work studied the reliability of NCF treated flip-chip package containing conventional solder bumps [1]-[5], [8], [9], [11], [12]. Copper pillar has various advantages over conventional solder bumps, e.g., higher thermal and electrical conductivity and efficient mechanical support [14]-[16]. Only limited studies evaluated the thermal cycling, moisture sensitivity and high temperature storage reliability reliabilities of solder bump and copper pillars [6], [10], [13]. The type of NCF and NCF compositions were not revealed in these reliability studies. Also, no explanation was given on how the NCF constituents

Saif Wakeel was with Centre of Advanced Materials, Department of Mechanical Engineering, Faculty of Engineering, University of Malaya, Kuala Lumpur 50603, Malaysia (e-mail: saifwakeel@gmail.com). He is currently with Photonic Packaging Group, Tyndall National Institute, Cork, Ireland (e-mail: saif.wakeel@tyndall.ie).

A.S.M.A. Haseeb is with Centre of Advanced Materials, Department of Mechanical Engineering, Faculty of Engineering, University of Malaya, Kuala Lumpur 50603, Malaysia (e-mail: haseeb@um.edu.my). He is currently at Department of Glass and Ceramic Engineering, Bangladesh University of Engineering and Technology (BUET), Dhaka, Bangladesh.

Khoo Ly Hoon is with Assembly Process Innovation, NXP Semiconductor Sdn. Bhd., Selangor, Malaysia (e-mail: rachel.khoo@nxp.com).

M.A. Amalina is with Department of Mechanical Engineering, Faculty of Engineering, University of Malaya, Kuala Lumpur 50603, Malaysia. (e-mail: amalina@um.edu.my).

© 2022 IEEE. Personal use is permitted, but republication/redistribution requires IEEE permission. See https://www.ieee.org/publications/rights/index.html for more information.
Authorized licensed use limited to: UNIVERSITY COLLEGE CORK. Downloaded on August 12,2022 at 14:49:25 UTC from IEEE Xplore. Restrictions apply.

This article has been accepted for publication in IEEE Transactions on Components, Packaging and Manufacturing Technology. This is the author's version which has not been fully edited content may change prior to final publication. Citation information: DOI 10.1109/TCPMT.2022.3191604

are affecting the reliability of the solder bump and copper pillar for fine pitch flip-chip packages.

In our previous work, the chemistry and thermal behavior of a commercial "extremely low" and a "low" residue NCF were investigated. Hygroscopicity and wetting of SAC305 solder were also evaluated. Further, the die pull strength of the flip-chip package prepared by these NCF was determined after the reflow. Die pull strength results showed that NCF performed better than WS, and NC-1 was better than NC-2 [17]. However, the die pull strength tests carried out after reflow may not be sufficient to judge the performance of the flip-chip package as these tests were performed typically on the same day as reflow.

Therefore, the objective of this study is to evaluate the effects of constituents of "extremely low" and "low" residue NCF on the moisture sensitivity (30 ºC/60% RH), thermal cycling (-65 ºC to 150 ºC), and thermal storage (175 ºC) reliabilities of fine pitch flip-chip package with solder bump and copper pillar. For comparison, one water-soluble flux was also used.

II. EXPERIMENTAL PROCEDURE

The constituents and viscosity of each flux, as per supplier data sheets, are presented in Table I. These fluxes were used to build fine pitch (150 µm) flip-chip package containing solder bump with copper pillar. From Table I, extremely low residue flux (NC-1) consists of hybrid monocarboxylic acid activator and tertiary amine. Low residue flux (NC-2) contains single monocarboxylic acid and secondary amide. The constituents of fluxes were originally revealed by the supplier, which were confirmed by our previous study [17].

A. Test Vehicle

These fluxes were used to build 17x17 mm^2 package using 7.6x7.6 mm^2 Si die. The thickness of the die was 295 µm and bump pitch was 150 µm. Dimension of package components are listed in Table II of our previous study [17] which is also presented in Table II of this study. To prepare this package, a low k, Cu pillar and Pb-free bump compatible underfill was applied. As per supplier data sheet, underfill used in this study was prepared using bisphenol F type liquid epoxy resin, amine type hardener, silicon dioxide filler (2-5 µm) and additives. The glass transition temperature (Tg) of underfill was 95 ºC. The viscosity, elastic modulus and CTE (<Tg) were 55 Pa.s, 12 GPa and 22 ppm/ ºC, respectively. Reflow of this package was performed at a ramping rate of 0.5 ºC/sec. The preheating was done from 100 ºC to 220 ºC. Time above liquidus temperature was 50-70 sec. with peak temperature range being 235-250 ºC [17].

B. Reliability tests

Curing of the underfill was done for 6 hours at 150 ºC. After curing, moisture sensitivity test was performed on 34 test vehicles as per JESD22-A113D [18]. Solder bump failure was not observed in the MSL test. Therefore, 32 test vehicles from the moisture sensitivity test were sent for thermal cycling test which was performed as per JESD22-A104D [19]. High-temperature storage life (HTSL) test was performed by following JESD22-A103C [20]. A total of 30 test vehicles were used for the HTSL test. Test conditions for each of the tests are given in Table III.

In MSL test, C-SAM of 100%-time zero (T0) test vehicles and post-MSL was done using advanced sonoscan by 20MHz transducer to observe delamination or underfill voids. In TC test, C-SAM of 100% test vehicles after 2000 cycles were conducted to observe the voids. C-SAM of all the test vehicles at time zero (T0), 512 hours, and 2016 hours was done in HTSL test. Failure of a test vehicle in C-SAM was defined as the "occurrence of at least a void with a size greater than two solder bump areas throughout the die area". The percentage of test vehicle failed was calculated using Equation 1.

In each reliability test, the two worst test vehicles were selected based on C-SAM images. These vehicles were molded in epoxy and hardener ratio of 2:15 and grinding of units was done by different SiC abrasive papers of 250, 400, 600, 800, 1200, 1500, and 3000 grits. Then, polishing of samples was done using 9,3 and 1 µm diamond suspension. To increase the accuracy of data, SEM images of die central, left, and right end layers were taken. In each layer, SEM images of 10 solder bumps were observed at 1000 and 2500x. EDX mapping was done to confirm the delamination at underfill/solder mask interface. In HTSL test, IMCs thicknesses on the copper pillar and copper pad side were measured at the four locations on each IMCs and 10 bumps were used for IMC measurement. Average of these thicknesses were done to calculate the final thickness.

III. RESULTS

A. Moisture sensitivity level reliability

Due to the proprietary reason, C-SAM images of die area cannot be included. From Equation 1, the number of test vehicles that failed before and after MSL was calculated and presented in Table IV. WS-based vehicles did not show any failure, but NCF vehicles had failure as listed in Table IV. After MSL, in NC-1 amount of vehicles failure (15.62%) was higher than NC-2 (3.10%). SEM images of solder bumps and underfill/solder mask interface before and after MSL are shown in Figure 1. From the SEM images presented in Figure 1 (a), (c), (e), all the solder bumps were fully formed, and scallop intermetallic Cu_6Sn_5 and Cu_3Sn were observed on the Cu pillar and Cu pad side at time zero. Further, different sizes of silica filler particles (2-5 µm) were uniformly distributed throughout the die area and no abnormalities were found at underfill/solder mask interface. After MSL, severe delamination at underfill/solder mask interface was noticed in presence of NCF residue as illustrated in Figure 1 (b), (d), (f). This was confirmed by the EDX mapping presented in Figure 2. From Figure 2, silicon (Si) and oxygen (O) were majorly found in underfill because silica (SiO_2) was the filler material as described in section 2.1. However, certain amount of tin (Sn) was found which is shown by white region between underfill and solder mask. Tin migration to this region confirms the delaminated area.

B. Thermal cycling reliability

© 2022 IEEE. Personal use is permitted, but republication/redistribution requires IEEE permission. See https://www.ieee.org/publications/rights/index.html for more information.
Authorized licensed use limited to: UNIVERSITY COLLEGE CORK. Downloaded on August 12,2022 at 14:49:25 UTC from IEEE Xplore. Restrictions apply.

This article has been accepted for publication in IEEE Transactions on Components, Packaging and Manufacturing Technology. This is the author's version which has not been fully edited content may change prior to final publication. Citation information: DOI 10.1109/TCPMT.2022.3191604

Based on the C-SAM images, the percentage of test vehicles failure was calculated using Equation 1 and is listed in Table V. NCF based assembly showed failure whereas, WS based cleaned assembly did not show any failure as described in Table V. For NCF, the percentage of units failed was increasing with the number of cycles. Also, NC-1 had higher number of failures as compared to NC-2. SEM images of die cross-section at time zero and after 2000 cycles are shown in Figure 3. Severe delamination was found for NC-1 and NC-2 as described in Figure 3. However, WS-based assemblies did not show any delamination after 2000 cycles. Breaking of solder bump was observed for NCF's. In addition, the crack was noticed after 500 cycles for NC-1 and 1500 cycles for NC-2, but the crack initiation cycle is not known as the data reading point was 500 cycles.

C. High temperature storage reliability

C-SAM images of all test vehicles were examined after 504 hours and 2016 hours. From Equation 1, the percentage of the vehicle failed is presented in Table VI. No failure was found in NCF's and WS-based test vehicles after 2016 hours, which is the maximum time period studied in this work. SEM images of selected vehicles for each flux are shown in Figure 4. All the solder bumps were fully formed at time zero and IMCs Cu_6Sn_5 and Cu_3Sn were observed on the copper pillar and pad side as reflected in Figure 4 (a), (c), (e). After 2016 hours, the thickness of IMC increased significantly as compared to time zero as presented in Figure 4 (b), (d), (f). The total IMCs thicknesses on Cu pillar and Cu pad sides were found to be similar for all the fluxes within the standard deviations. Maximum IMCs thickness for each flux at time zero was 5.70 µm and after 2016 hours the maximum thickness was found to be 27.32 µm. Thus, the fluxes did not have any detectable effect on IMCs.

IV. DISCUSSION

Results of the MSL test (Table IV) showed that after underfill curing and before the MSL test, no failure or delamination was observed by C-SAM images for any of the fluxes. This was further confirmed by SEM (Figure 1). However, C-SAM images after 3x reflow in the MSL test showed significant failure of the test vehicles which was also verified by SEM. Delamination at underfill-solder mask interface is found for samples prepared by NCF. WS assembly, on the other hand, does not show any delamination. An important factor affecting the underfill delamination is the interaction between NCF residue and underfill [33]. The residues of the NCF were found to be hygroscopic in our previous study [17]. Thus, absorbed moisture is likely to hinder the adhesion of underfill to critical locations such as solder mask, corner of solder bumps etc. During the reflow stage (3x at 260 °C) of MSL, the moisture could have expanded (popcorning) leading to the formation of voids or delamination. Thus, it is suggested that reduction in underfill adhesion in presence of NCF residue led to the failure of the package [21]-[25]. Fan et al. [4] observed the decrease in the adhesion strength of three underfill due to moisture absorption during reflow (220 °C) stage of MSL in presence of NCF residue. Similar results were found in [1], [2] in which underfill voids and delamination were observed during the reflow (260 °C) stage of MSL due to the popcorning of moisture absorbed by NCF. Besides, delamination can also occur due to a reduction in the degree of curing, and a reduction in glass transition temperature and elastic modulus of the epoxy underfill by monocarboxylic acids based NCF residue [26]-[28]. The presence of solder was identified in the crevices in delaminated areas by EDX mapping as described in section III.A. During the 3x reflow, adhesion of underfill to the solder mask was compromised in presence of NCF residue (as discussed earlier). Thus, solder migrated to that weakened space between underfill and solder mask. Baldwin et al. [29] observed that delamination happened during the reflow stage of MSL and then molten solder migrated to this delaminated area. Similar failure was observed by others [30, 31].

Results of the MSL test of flip-chip package using no-clean flux have been compared with the studies reported in the literature. A few previous studies used similar test conditions (30 °C /60% RH, 192 hrs and 3x reflow at 260 °C) as employed in this study [2], [3], [4]. Results of these studies showed that in the presence of NCF residue, failure of test vehicles was found by C-SAM. In this work, failure was also detected using C-SAM images and NC-1 showed a greater number of test vehicles failure than NC-2. Some other studies used more aggressive test conditions such as 121 °C/100%RH, reflow 3x at 220 °C and 30/70% RH, 120 hrs, 3x reflow at 240 [1], [5]. They found the failure of test vehicles containing NCF using C-SAM images. Therefore, NCF based test vehicles showed failure in mildly and highly aggressive conditions of MSL.

In thermal cycling, the WS treated test vehicles did not show any delamination or solder bump crack. Solder bump cracks for NC-1 occurred at <500 cycles whereas, that for NC-2 happened at <1500 cycles. During the thermal cycling, delamination of underfill can lead to solder cracking. Because of delamination, stresses on the solder joints are redistributed. In presence of underfill delamination, maximum von mises stress was found to have increased by 83% as compared to the non-failure case [32]. Stress redistribution is suggested to lead to the cracking of solder bumps as shown in Figure 3.

The properties of underfill epoxy are also influenced by the type of carboxylic acid. For example, a reduction in the degree of curing, glass transition temperature, elastic modulus, and storage property of epoxy resin in an acidic environment is affected by the chain length of the acid. Previous studies showed that increasing the chain length of dicarboxylic acid will decrease the degree of curing, glass transition temperature, elastic modulus, and storage property of epoxy resin used in the underfill. This is because an increase in steric effect will hinder the formation and cross-linking between microgels particles [26]-[28]. However, these studies have been performed only for dicarboxylic acids but not extended to monocarboxylic acids used in our study. NC-1 contains monocarboxylic acids with the chain length of C8:C10:C12 whereas, the chain length of acid in NC-2 is C3. Thus, it is suggested that lower chain length can be another reason for localized delamination of underfill in presence of residue of NC-2. In NC-1, trihexylamine (a tertiary amine) is used as an adhesion promoter as presented in Table I. NC-2 contains polyethyleneamine-polyamide (secondary amide) as an adhesion promoter. The primary function of an

© 2022 IEEE. Personal use is permitted, but republication/redistribution requires IEEE permission. See https://www.ieee.org/publications/rights/index.html for more information.
Authorized licensed use limited to: UNIVERSITY COLLEGE CORK. Downloaded on August 12,2022 at 14:49:25 UTC from IEEE Xplore. Restrictions apply.

This article has been accepted for publication in IEEE Transactions on Components, Packaging and Manufacturing Technology. This is the author's version which has not been fully edited content may change prior to final publication. Citation information: DOI 10.1109/TCPMT.2022.3191604

adhesion promoter is to increase the adhesion of NCF with underfill [33]. Secondary amide used in NC-2 reacts with the epoxy and a ring-opening reaction occurs. This is a curing reaction of epoxy in presence of cross-linking agent and this reaction is based on hydrogen bond donation tendency. The proposed reaction of the amide with epoxy is given in Figure 5 [34], [35].

Polyamide reacts with the epoxy and cross-linking of epoxy chain occurs and forms hydroxyl products of amide as seen in Figure 5. Amide can cure the epoxy in highly rigid plasticized thermosetting polymer which has higher adhesion strength [35], [36]. Therefore, it is suggested that this reaction increases the compatibility between NC-2 residue and underfill epoxy which makes the solder bump survive at <1500 cycles. However, tertiary amine does not have any hydrogen bond and hence there is no reaction between tertiary amine and epoxy underfill [34], [36]. The residue of NC-1 is non-reactive with epoxy underfill as tertiary amine is found in its residue. This non-reactive residue will be carried out by underfill during dispensing, and it will interrupt the underfill adhesion on critical locations such as corners of the solder bump, the opposite end of underfill dispense, etc. [33]. Thus, higher thermal stress transfer will lead to cracking of solder bump at <500 cycles.

A comparison of the thermal cycling reliability results is done with the results of the current study in Table VII. Previous studies listed in Table VII show that under less severe (-40 ºC to 115 ºC, -40 ºC to 125 ºC) and mildly severe (-55 ºC to 125 ºC) conditions NCF based assemblies survived 1000 cycles in the TC tests [5], [8], [9], [11]. However, constituents of the NCF were not revealed in these studies. In the present study, NC-1 based assembly passed <500 cycles whereas, NC-2 based assembly could pass <1500 cycles. The much shorter lifetime NC-1 in this study can be attributed to the two possible reasons. In the present study, the package is tested under extreme temperature conditions of -65 ºC to 150 ºC which is severe than those employed in previous studies as shown in Table VII. Secondly, the constituents of NC-1 such as carboxylic acid activator and amine adhesion promoter might have a significant effect on the properties and adhesion of underfill during the thermal cycling test as explained earlier. The performance of NC-2 (< 1500 cycles) seems reasonable compared with data presented in the literature. WS obviously performed better (> 2000 cycles) compared with both NC-1 and NC-2.

In earlier studies, high-temperature storage test was performed at 150 ºC. Their results showed that in presence of NCF residue, no crack on die, underfill, and solder were found until 2000 hours. Thicker IMCs (Cu_6Sn_5 and Cu_3Sn) were seen after 2000 hours but thickness data is not available [10], [13]. The thermal storage test in this study was performed at 175 ºC which is significantly higher than those employed in previous tests. After 2016 hours, solder cracking was not found and 100% of the test vehicles survived for no clean and water-soluble fluxes.

V. Conclusions

Based on the results presented, the major conclusions are as follows:

- C-SAM data after moisture sensitivity test showed that the percentage failure for NC-1 was 15.62% and NC-2 was 3.10%, while WS cleaned assembly did not show any failure. Further, SEM images and EDX mapping showed delamination of underfill from solder mask surface for NCF, but no delamination was found for WS treated assembly. These results were attributed to the hygroscopic residue of NCF. Also, underfill properties such as glass transition temperature, elastic modulus etc. were believed to have been impacted negatively by type of carboxylic acid used for NCF preparation.
- Percentage failure of packages prepared by using NCF was increased with number of cycles. After 2000 cycle, 19.96% of total units failed in presence of NC-1 residue and 7.26% units for residue of NC-2. Whereas packages prepared by using WS did not show any failure. Solder bump crack occurred at <500 cycles for NC-1 and at <1500 cycles for NC-2. In addition to the type of carboxylic acid used, polyamide adhesion promoter was suggested to have induced favorable reactions between NC-2 with underfill which led the solder bump survive for up to <1500 cycles. In NC-1, trihexylamine was used as an adhesion promoter which did not react with underfill thus, led the solder bump cracking in <500 cycles.
- The findings of this study showed that no-clean flux treated packages performed worse than those prepared with water-soluble flux. Therefore, more attention needs to be done when preparing the flip-chip package using no-clean fluxes as they might not perform adequately, particularly under severe conditions. There are scopes for packaging materials industry to improve NCF performance by optimizing the constituents of no-clean fluxes such as the suitable combination of shorter chain length monocarboxylic acids, secondary amide/amine, etc.

References

1. Todd, M., & Costello, K. (2001, March). No-Clean assembly process conditions-effects on flip-chip/underfill reliability. In Proceedings International Symposium on Advanced Packaging Materials Processes, Properties and Interfaces (IEEE Cat. No. 01TH8562) (pp. 42-45). IEEE.
2. Toleno, B. J., & Carson, G. (2004). Flip chip underfill and flux residue with Lead free. Circuits Assembly, 15, 24-29.
3. Ong, Y. Y., Vaidyanathan, K., Ho, S. W., Sekhar, V. N., Jong, M. C., Wai, L. C., ... & Sohn, D. K. (2008, December). Design, Assembly and Reliability of Large Die (21 x 21mm2) and Fine-pitch (150pm) Cu/Low-K Flip Chip Package. In 2008 10th Electronics Packaging Technology Conference (pp. 613-619). IEEE.
4. Fan, X. J., Tee, T. Y., Cui, C. Q., & Zhang, G. Q. (2010). Underfill selection against moisture in flip chip BGA packages. In Moisture Sensitivity of Plastic Packages of IC Devices (pp. 435-460). Springer, Boston, MA.
5. Wang, T., Tung, F., Foo, L., & Dutta, V. (2001, May). Studies on a novel flip-chip interconnect structure. Pillar bump. In 2001 Proceedings. 51st Electronic Components and Technology Conference (Cat. No. 01CH37220) (pp. 945-949). IEEE.
6. Wang, T., Tung, F., Foo, L., & Dutta, V. (2001, May). Studies on a novel flip-chip interconnect structure. Pillar bump. In 2001 Proceedings. 51st Electronic Components and Technology Conference (Cat. No. 01CH37220) (pp. 945-949). IEEE.
7. Libres, J., & Arroyo, J. C. (2010, June). Investigation of bump crack and deformation on Pb-free flip chip packages. In 2010 Proceedings

© 2022 IEEE. Personal use is permitted, but republication/redistribution requires IEEE permission. See https://www.ieee.org/publications/rights/index.html for more information.
Authorized licensed use limited to: UNIVERSITY COLLEGE CORK. Downloaded on August 12,2022 at 14:49:25 UTC from IEEE Xplore. Restrictions apply.

This article has been accepted for publication in IEEE Transactions on Components, Packaging and Manufacturing Technology. This is the author's version which has not been fully edited content may change prior to final publication. Citation information: DOI 10.1109/TCPMT.2022.3191604

60th Electronic Components and Technology Conference (ECTC) (pp. 1536-1540). IEEE.
8. Ho, P. S., Xiong, Z. P., & Chua, K. H. (2007, December). Study on factors affecting underfill flow and underfill voids in a large-die flip chip ball grid array (FCBGA) package. In 2007 9th Electronics Packaging Technology Conference (pp. 640-645). IEEE.
9. Horibe, A., Lee, K. W., Okamoto, K., Mori, H., Orii, Y., Nishizako, Y., ... & Shirai, Y. (2013, May). No clean flux technology for large die flip chip packages. In 2013 IEEE 63rd Electronic Components and Technology Conference (pp. 688-693). IEEE.
10. Orii, Y., Toriyama, K., Noma, H., Oyama, Y., Nishiwaki, H., Ishida, M., ... & Feger, C. (2009, May). Ultrafine-pitch C2 flip chip interconnections with solder-capped Cu pillar bumps. In 2009 59th electronic components and technology conference (pp. 948-953). IEEE.
11. Ong, Y. Y., Ho, S. W., Vaidyanathan, K., Sekhar, V. N., Jong, M. C., Long, S. L. Y., ... & Sohn, D. K. (2010). Design, assembly and reliability of large die and fine-pitch Cu/low-k flip chip package. Microelectronics Reliability, 50(7), 986-994.
12. Tsai, W. M., Houston, P. N., & Baldwin, D. F. (2000, October). Flux-underfill compatibility and failure mode analysis in high yield flip chip processing. In Twenty Sixth IEEE/CPMT International Electronics Manufacturing Technology Symposium (Cat. No. 00CH37146) (pp. 160-167). IEEE.
13. Orii, Y., Toriyama, K., Kohara, S., Noma, H., Okamoto, K., Toyoshima, D., & Uenishi, K. (2011). Micro structure observation and reliability behavior of peripheral flip chip interconnections with solder-capped Cu pillar bumps. Transactions of The Japan Institute of Electronics Packaging, 4(1), 73-86.
14. Huang, M. L., Zhang, F., Yang, F., & Zhao, N. (2015). Size effect on tensile properties of Cu/Sn–9Zn/Cu solder interconnects under aging and current stressing. Journal of Materials Science: Materials in Electronics, 26(4), 2278-2285.
15. Yoo, Y. R., & Kim, Y. S. (2010). Influence of electrochemical properties on electrochemical migration of SnPb and SnBi solders. Metals and Materials International, 16(5), 739-745.
16. Lee, C. H. (2009, June). Interconnection with Copper Pillar Bumps: process and applications. In 2009 IEEE International Interconnect Technology Conference (pp. 214-216). IEEE.
17. Wakeel, S., Haseeb, A. S. M. A., Afifi, M. A., & Hoon, K. L. (2021). Investigation into chemistry and performance of no-clean flux in fine pitch flip-chip package. IEEE Transactions on Components, Packaging and Manufacturing Technology. DOI: 10.1109/TCPMT.2021.3109885.
18. JEDEC standard 22-A101-B, (1997). Steady state temperature humidity biased test. http://web.cecs.pdx.edu/~cgshirl/Documents/22a101b%208585.pdf
19. JEDEC standard 22-A104-B, (2000). Temperature cycling. http://web.cecs.pdx.edu/~cgshirl/Documents/22a104b%20Temperature%20Cycling.pdf
20. JEDEC standard 22-A103D, (2010). High temperature storage life. https://www.jedec.org/sites/default/files/docs/22a103D.pdf
21. Ferguson, T., & Qu, J. (2002). Effect of moisture on the interfacial adhesion of the underfill/solder mask interface. *J. Electron. Packag.*, *124*(2), 106-110.
22. Okura, J. H., Dasgupta, A., & Caers, J. F. J. M. (2002). Hygro-mechanical durability of underfilled flip-chip-on-board (FCOB) interconnects. *J. Electron. Packaq.*, *124*(3), 184-187.
23. Fan, X., Zhang, G. Q., Van Driel, W. D., & Ernst, L. J. (2008). Interfacial delamination mechanisms during soldering reflow with moisture preconditioning. *IEEE Transactions on Components and Packaging Technologies*, *31*(2), 252-259.
24. Kwei, T. K. (1966). Strength of epoxy polymers. I. Effect of chemical structure and environmental conditions. *Journal of Applied Polymer Science*, *10*(11), 1647-1655.
25. Xiao, G. Z., & Shanahan, M. E. R. (1998). Swelling of DGEBA/DDA epoxy resin during hygrothermal ageing. *Polymer*, *39*(14), 3253-3260.
26. Hong, C., Wang, X., Pan, Z., & Zhang, Y. (2015). Curing thermodynamics and kinetics of unsaturated polyester resin with different chain length of saturated aliphatic binary carboxylic acid. Journal of Thermal Analysis and Calorimetry, 122(1), 427-436.
27. Choi, M. H., Byun, H. Y., & Chung, I. J. (2002). The effect of chain length of flexible diacid on morphology and mechanical property of modified phenolic resin. Polymer, 43(16), 4437-4444.
28. Smith, J. D., & Kauffman, R. N. (1977). U.S. Patent No. 4,026,862. Washington, DC: U.S. Patent and Trademark Office.
29. Baldwin, D. F., Houston, P. N., Deladisma, M., Crane, L. N., & Konarski, M. M. (2000). Processing and reliability of fast-flow, snap-cure underfills. I. Processing and moisture sensitivity. *IEEE Transactions on Electronics Packaging Manufacturing*, *23*(4), 259-266.
30. Bernard, D., & Willis, B. (2005). Correlating the Presence of Popcorned BGA Devices Post Reflow with Solder-Ball Diameter Measurements from X-ray Inspection. *Proceedings of SMTA International, Chicago*.
31. Houston, P. N., Baldwin, D. F., Deladisma, M., Crane, L. N., & Konarski, M. (1999). Processing and Reliability of Low Cost Flip Chip Assemblies Implementing Fast-Flow, Snap-Cure Underfills. In *Proc. 48 th SMTA Conference & Exposition*.
32. Fan, X. J., Wang, H. B., & Lim, T. B. (2001). Investigation of the underfill delamination and cracking in flip-chip modules under temperature cyclic loading. *IEEE Transactions on Components and Packaging Technologies*, *24*(1), 84-91.
33. Wakeel, S., Haseeb, A. S. M. A., Afifi, M. A., Bingol, S., & Hoon, K. L. (2021). Constituents and performance of no-clean flux for electronic solder. Microelectronics Reliability, 123, 114177.
34. Blank, W. J., He, Z. A., & Picci, M. (2002). Catalysis of the epoxy-carboxyl reaction. Journal of Coatings Technology, 74(926), 33-41.
35. Applied poleramic, (2015). AMINE CURED-EPOXY MATRICES. http://www.appliedpoleramic.com/wp-content/uploads/2015/05/API-TECH-NOTE-2-Amine-Cured-Epoxy-Matrices.pdf
36. Ashcroft, W. R. (1993). Curing agents for epoxy resins. In Chemistry and technology of epoxy resins (pp. 37-71). Springer, Dordrecht.



Saif Wakeel received the B.Tech. degree (Hons.) in mechanical engineering from Aligarh Muslim University, Aligarh, India, in 2018 and Master of Engineering Science by Research degree with the University of Malaya, Kuala Lumpur, Malaysia. He is currently pursuing Ph.D. from Tyndall National Institute, University College Cork, Ireland. He was a Research and Development Intern at NXP Semiconductors, Malaysia, for two years during his master's degree. He has completed eight months Erasmus+ fellowship program at Dicle Universitesi, Diyarbakir, Turkey. He was a Research Intern at the National University of Singapore (NUS), Singapore. His research interests include characterization and reliability of fine pitch flip-chip packaging and related materials, wafer level photonic packaging, radio frequency packaging. He has authored several publications, and two invited books. He is a six-sigma yellow belt holder.



A. S. M. A. Haseeb (Member, IEEE) received the bachelor's and master's degrees in metallurgical engineering from Bangladesh University of Engineering and Technology (BUET), Dhaka, Bangladesh, in 1984 and 1986, respectively, and the Ph.D. degree in materials engineering from the Catholic University of Leuven (KU Leuven), Leuven, Belgium, in 1992. He is currently working as a Professor with the Department of Mechanical Engineering, Faculty of Engineering, University of Malaya (UM), Kuala Lumpur, Malaysia. His current research interests include electronic

© 2022 IEEE. Personal use is permitted, but republication/redistribution requires IEEE permission. See https://www.ieee.org/publications/rights/index.html for more information.
Authorized licensed use limited to: UNIVERSITY COLLEGE CORK. Downloaded on August 12,2022 at 14:49:25 UTC from IEEE Xplore. Restrictions apply.

This article has been accepted for publication in IEEE Transactions on Components, Packaging and Manufacturing Technology. This is the author's version which has not been fully edited content may change prior to final publication. Citation information: DOI 10.1109/TCPMT.2022.3191604

packaging materials, nanostructures for gas sensing applications, and degradation of materials in a hostile environment. Dr. Haseeb is a fellow of the Institute of Mechanical Engineers (IMechE), U.K., and a Chartered Engineer of the Engineering Council, U.K. He is also a member of The Minerals, Metals & Materials Society (TMS), USA. He is also the Editor-in-Chief of the Encyclopedia of Materials: Electronics (Elsevier).



M. A. Amalina received the B.Eng. and M.Eng. degrees in polymer science and engineering and the D.Eng. degree in materials and life science Kyoto Institute of Technology (KIT), Kyoto, Japan, in 2000, 2002, and 2010, respectively. She then continued her doctoral study after 5 years working with the Department of Mechanical Engineering, University Malaya (UM), Kuala Lumpur, Malaysia. She did her post-doctoral research at Helmholtz-Zentrum Geesthacht, Geesthacht, Germany, in 2014. She is currently working as an Associate Professor at the Department of Mechanical Engineering, Faculty of Engineering, UM. Her current research interest is in developing chitosan as materials for various applications, such as biomedical material, membrane for water/wastewater treatment, or electronic material.



Khoo Ly Hoon received the B.S degree in material engineering from the National University of Malaysia, Bangi, Malaysia, in 2007. She currently works as a Staff IC Packaging Development Engineer with the Research and Development Department, NXP Semiconductor Malaysia, Petaling Jaya, Malaysia. She has experience in assembly processes, such as laser groove, dicing, die sort, die bond, underfill, and curing. She is the inventor or the co-inventor of seven inventions.

$$\text{Percentage number of test vehicles failure} = \frac{\text{The number of test vehicles with at least one void greater than two solder bump area}}{\text{The total number of test vehicles in the reliability test}} \times 100 \quad (1)$$

© 2022 IEEE. Personal use is permitted, but republication/redistribution requires IEEE permission. See https://www.ieee.org/publications/rights/index.html for more information.
Authorized licensed use limited to: UNIVERSITY COLLEGE CORK. Downloaded on August 12,2022 at 14:49:25 UTC from IEEE Xplore. Restrictions apply.

This article has been accepted for publication in IEEE Transactions on Components, Packaging and Manufacturing Technology. This is the author's version which has not been fully edited content may change prior to final publication. Citation information: DOI 10.1109/TCPMT.2022.3191604

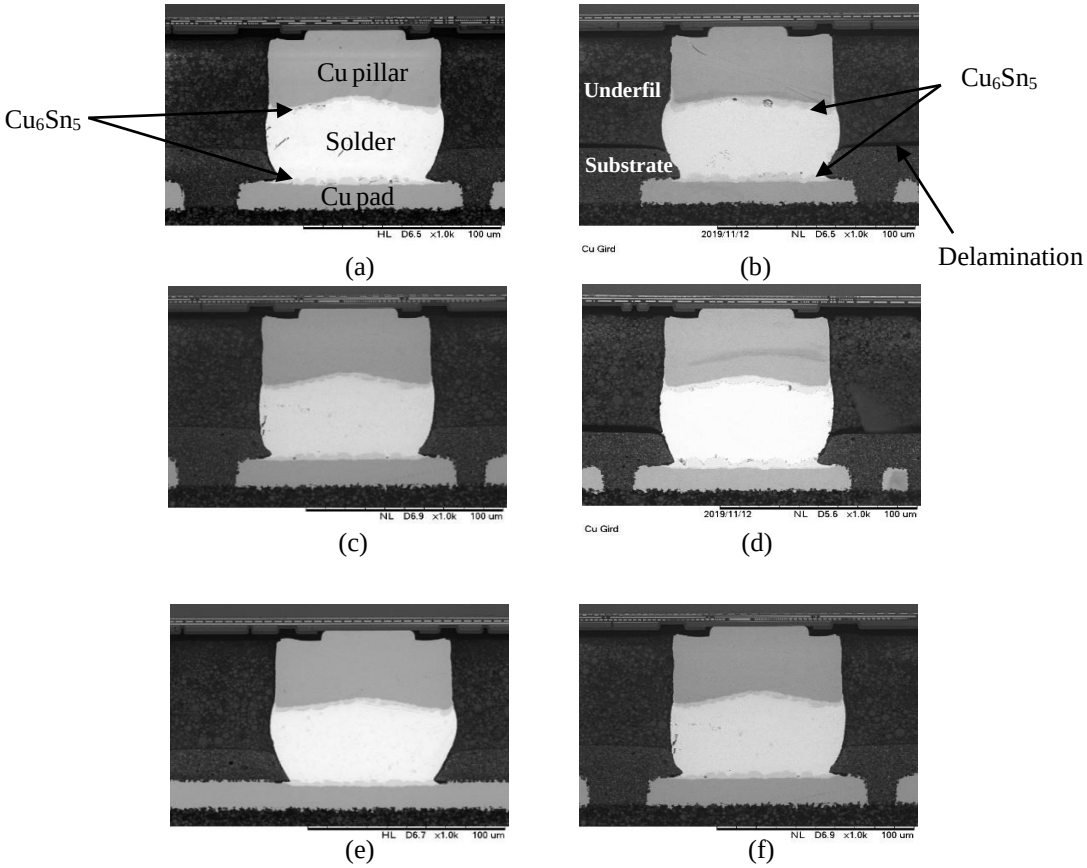


Figure 1: Cross sectional SEM images of the package. (a), (c), (e) are for NC-1, NC-2 and WS respectively before MSL test, and (b), (d), (f) for NC-1, NC-2 and WS respectively after MSL test.

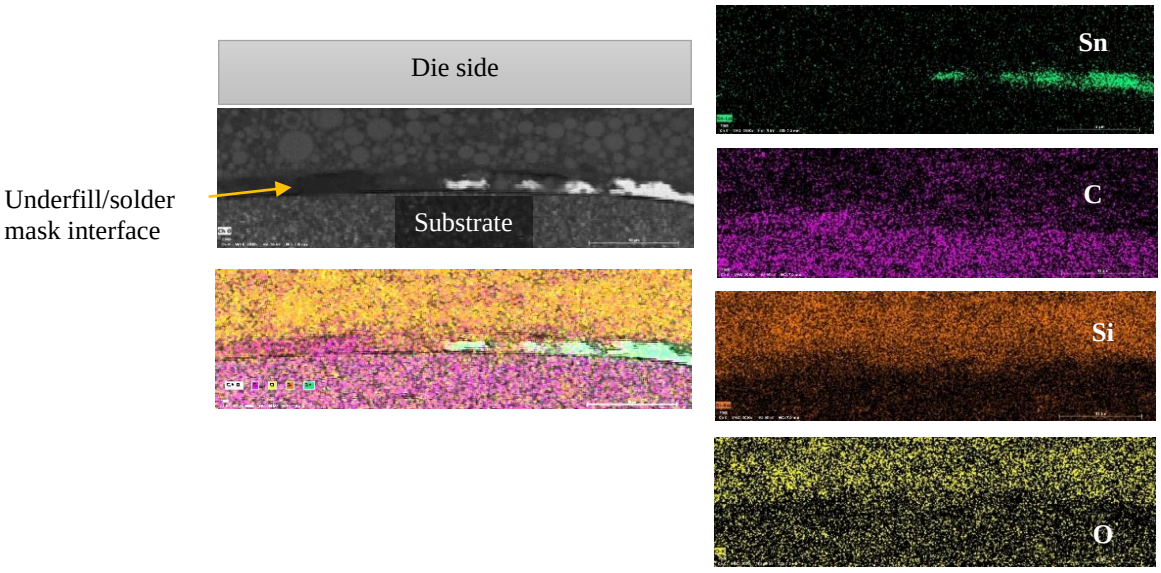


Figure 2: EDX area maps of underfill/solder mask interface.

© 2022 IEEE. Personal use is permitted, but republication/redistribution requires IEEE permission. See https://www.ieee.org/publications/rights/index.html for more information.
Authorized licensed use limited to: UNIVERSITY COLLEGE CORK. Downloaded on August 12,2022 at 14:49:25 UTC from IEEE Xplore. Restrictions apply.

This article has been accepted for publication in IEEE Transactions on Components, Packaging and Manufacturing Technology. This is the author's version which has not been fully edited content may change prior to final publication. Citation information: DOI 10.1109/TCPMT.2022.3191604

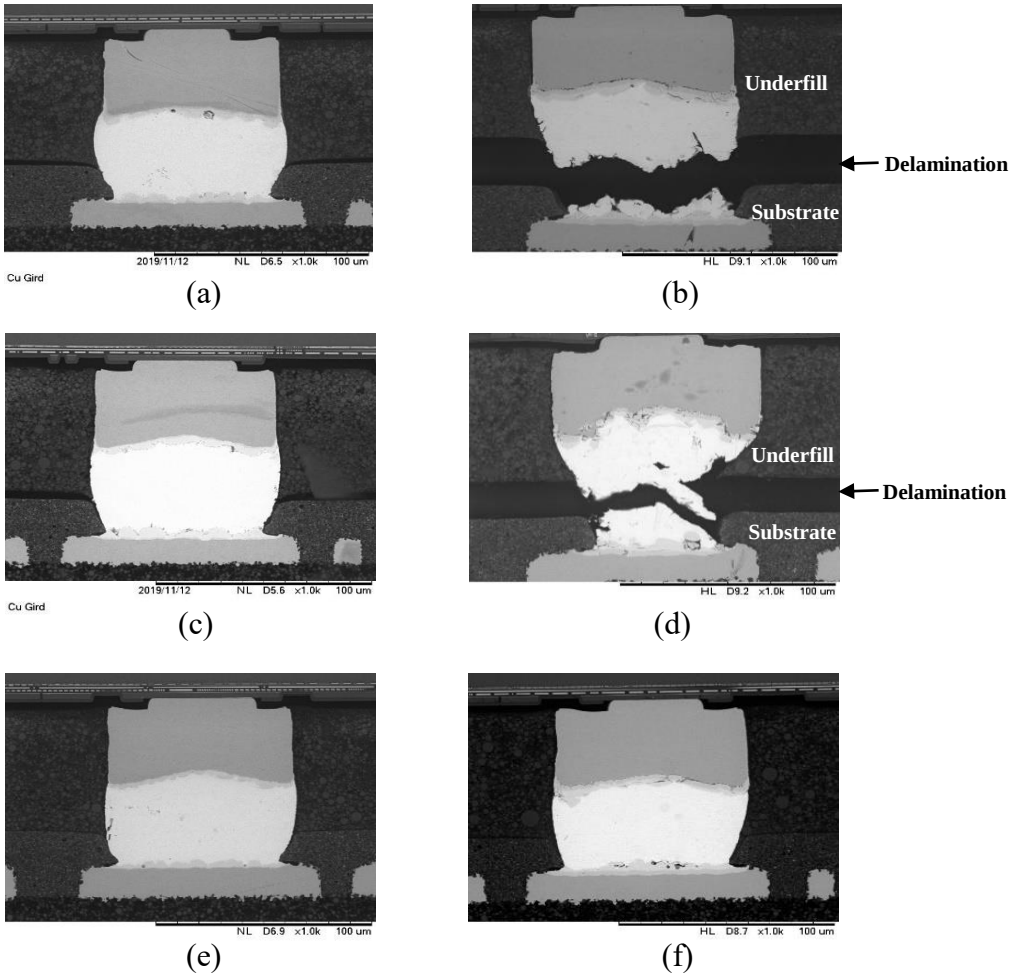


Figure 3: Cross sectional SEM images of the package. (a), (c), (e) are for NC-1, NC-2 and WS respectively at time zero, and (b), (d), (f) for NC-1, NC-2 and WS respectively after 2000 cycles.

© 2022 IEEE. Personal use is permitted, but republication/redistribution requires IEEE permission. See https://www.ieee.org/publications/rights/index.html for more information.
Authorized licensed use limited to: UNIVERSITY COLLEGE CORK. Downloaded on August 12,2022 at 14:49:25 UTC from IEEE Xplore. Restrictions apply.

This article has been accepted for publication in IEEE Transactions on Components, Packaging and Manufacturing Technology. This is the author's version which has not been fully edited content may change prior to final publication. Citation information: DOI 10.1109/TCPMT.2022.3191604

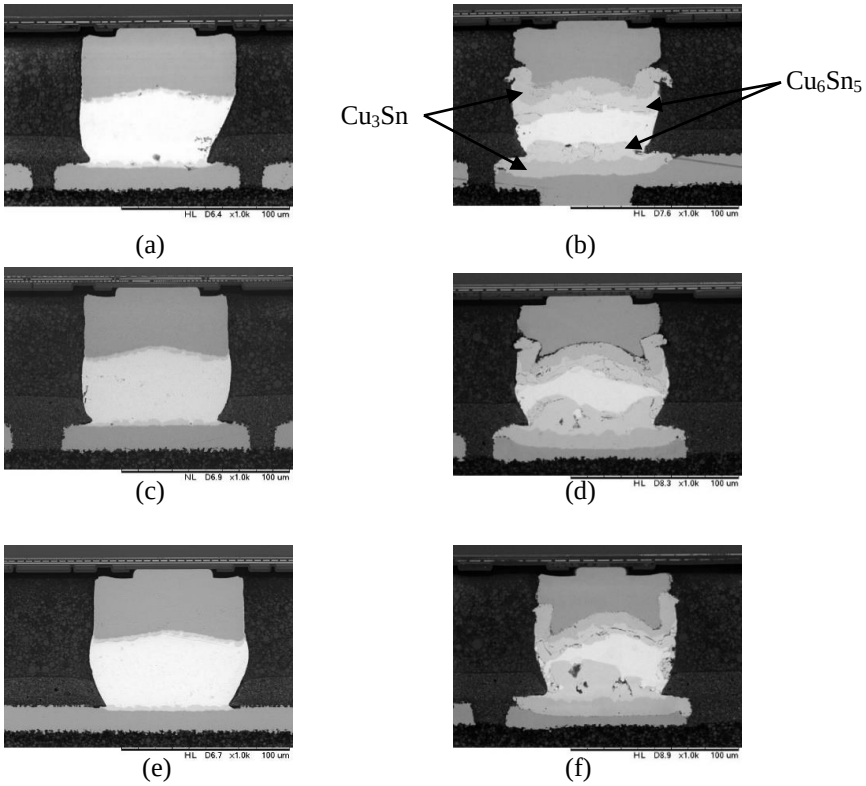


Figure 4: Cross sectional SEM images of the package. (a), (c), (e) are for NC-1, NC-2 and WS respectively at time zero, and (b), (d), (f) for NC-1, NC-2 and WS respectively after 2016 hours.

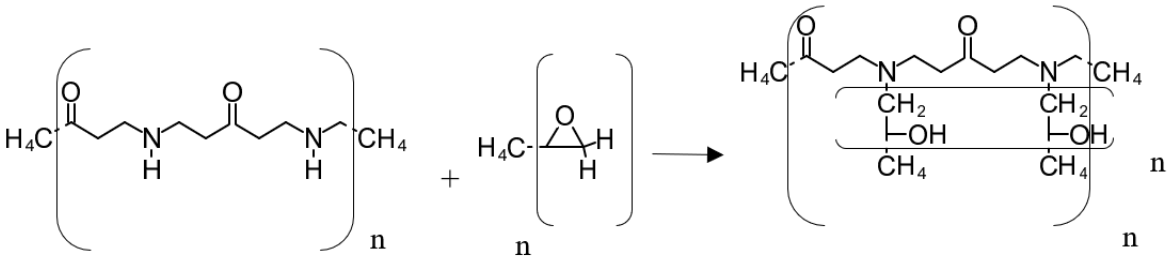


Figure 5: Ring opening reaction of secondary polyamide with epoxy [36].

TABLE I
MAJOR CONSTITUENTS AND VISCOSITY OF FLUXES.

Solder flux	Activator	Organic additive	Viscosity (cps)
NC-1	Caprylic acid + capric acid + lauric acid	Trihexylamine	1475
NC-2	Propionic acid	Polyethylenimine polyamide	13000
WS	Diglycolic acid	Polyoxypropylene ethylene diamine	20,000

© 2022 IEEE. Personal use is permitted, but republication/redistribution requires IEEE permission. See https://www.ieee.org/publications/rights/index.html for more information.
Authorized licensed use limited to: UNIVERSITY COLLEGE CORK. Downloaded on August 12,2022 at 14:49:25 UTC from IEEE Xplore. Restrictions apply.

This article has been accepted for publication in IEEE Transactions on Components, Packaging and Manufacturing Technology. This is the author's version which has not been fully edited content may change prior to final publication. Citation information: DOI 10.1109/TCPMT.2022.3191604

TABLE II
COMPONENTS OF PACKAGE AND THEIR DIMENSIONS

Package Component	Dimension (μm)
Die thickness	295
Cu pillar diameter	107.06 ± 2.59
Cu pillar height	34 ± 3.18
Sn2.5Ag cap height	16.5 ± 1.08
SAC305 pad height	16.3 ± 1.71
SAC305 diameter	74.13 ± 2.28
Bump pitch	150

TABLE III
RELIABILITY CONDITIONS USED IN THIS STUDY.

Reliability tests	Reliability conditions	Standard
Moisture sensitivity (MSL)	30 ºC/60% RH, 192 hours followed by 3x reflow at peak temperature of 260 ºC	JESD22-A113D
Thermal cycling (TC)	-65 ºC to +150 ºC, 2000 cycles (500 cycles as a read point)	JESD22-A104D
High temperature storage life (HTSL)	175 ºC, 2016 hours (512 hours as a read point)	JESD22-A103C

TABLE IV
PERCENTAGE NUMBER OF TEST VEHICLES FAILURE IN MOISTURE SENSITIVITY TEST.

Condition	NC-1 (%)	NC-2 (%)	WS (%)
Before MSL	0	0	0
After MSL	15.62	3.10	0

TABLE V
PERCENTAGE TEST VEHICLES FAILURE IN THERMAL CYCLING TEST.

Number of cycles	NC-1 (%)	NC-2 (%)	WS (%)
0	15.62	3.10	0
500	17.16	4.86	0
1000	18.90	5.78	0
2000	19.96	7.26	0

TABLE VI
PERCENTAGE FAILURE USING C-SAM IN HIGH TEMPERATURE STORAGE TEST.

Storage time	NC-1 (%)	NC-2 (%)	WS cleaned (%)
0	0	0	0
512	0	0	0
2016	0	0	0

TABLE VII
COMPARISON OF THERMAL CYCLING RESULTS OF THIS STUDY WITH PREVIOUS STUDIES.

Temperature cycling conditions (ºC)	Package size (mm x mm) and pitch (μm)	Flux constituents	Solder type	Number of cycles survived	Reference
-40 to 125	10 x 10 and 200	N.A.	SnAg	1000	[7]
-40 to 115	12.8 x 12.8 and 80, 50	N.A.	Sn2.5Ag	2250: for 80 μm 2000: for 50 μm	[11]
-55 to 125	21 x 21 and 150	N.A.	Sn3.5Ag, Sn2.5Ag and Sn37Pb	1000	[12]

© 2022 IEEE. Personal use is permitted, but republication/redistribution requires IEEE permission. See https://www.ieee.org/publications/rights/index.html for more information.
Authorized licensed use limited to: UNIVERSITY COLLEGE CORK. Downloaded on August 12,2022 at 14:49:25 UTC from IEEE Xplore. Restrictions apply.

This article has been accepted for publication in IEEE Transactions on Components, Packaging and Manufacturing Technology. This is the author's version which has not been fully edited content may change prior to final publication. Citation information: DOI 10.1109/TCPMT.2022.3191604

-55 to 125	19.7 x 19.7 and 200	N.A.	Sn/Pb	1000	[9]
-55 to 125	47.5 x 47.5 and 150	Rosin, Organic acid, amine haloid, alcohol/ether	SnAg	1000	[10]
-55 to 125	14.6 x 7.6	N.A.	Sn2.5Ag	2983	[8]
-65 to 150	17 x 17 and 150	Monocarboxylic acids, tertiary amine, secondary amide, monobutyl ether	Sn2.5Ag, SAC305	NC-1 <500 NC-2 <1500 WS >2000	[This study]

.

© 2022 IEEE. Personal use is permitted, but republication/redistribution requires IEEE permission. See https://www.ieee.org/publications/rights/index.html for more information.
Authorized licensed use limited to: UNIVERSITY COLLEGE CORK. Downloaded on August 12,2022 at 14:49:25 UTC from IEEE Xplore. Restrictions apply.